Successive passaging of the scrapie strains, ME7-ha and 139A-ha, generated by the interspecies transmission of mouse-adapted strains into hamsters markedly shortens the incubation times, but maintains their molecular and pathological properties

QI SHI[1*], KANG XIAO[1*], BAO-YUN ZHANG[1*], XIAO-MEI ZHANG[1], LI-NA CHEN[1], CAO CHEN[1], CHEN GAO[1] and XIAO-PING DONG[1,2]

[1]State Key Laboratory for Infectious Disease Prevention and Control, Collaborative Innovation Center for Diagnosis and Treatment of Infectious Diseases (Zhejiang University), National Institute for Viral Disease Control and Prevention, Chinese Center for Disease Control and Prevention, Beijing 102206; [2]Chinese Academy of Sciences Key Laboratory of Pathogenic Microbiology and Immunology, Institute of Microbiology, Chinese Academy of Sciences, Beijing 100101, P.R. China

Received July 7, 2014; Accepted February 10, 2015

DOI: 10.3892/ijmm.2015.2102

Abstract. As a type of zoonotic disease, prion diseases may be transmited naturally and experimentally among species. In a previous study, we demonstrated that the mouse-adapted scrapie strains, ME7 (ME7-mo) and 139A (139A-mo), can overcome the species barrier and induce experimental scrapie when inoculated into Golden hamsters and generated 2 new hamster-adapted strains, ME7 (ME7-ha) and 139A (139A-ha). In the present study, in order to assess the infectivity and other molecular and neuropathological properties of the newly formed scrapie agents, ME7-ha and 139A-ha were further intracerebrally inoculated into hamsters. Compared with infection with 1st passage strains, the incubation times and clinical courses of infection with 2nd passage strains were markedly shorter, which were quite comparable with those of the mice infected with their parent mouse strains. The glycosylation patterns of brain PrP^{Sc} in the animals infected with the 2nd passage of those 2 strains maintained similar features as those in the animals infected with the 1st passage of those strains, with predominantly diglycosylated PrP^{Sc}. Neuropathological assays revealed comparable spongiform degeneration and microglia proliferation in the brain tissues from the infected mice and hamsters, but markedly more plaque-like deposits of PrP^{Sc} and more severe astrogliosis in the brains of the hamster. These data indicate that the strains, ME7-ha 1st and 139A-ha 1st generated by interspecies infection can passage in the new host hamster and stably maintain their molecular and neuropathological characteristics.

Correspondence to: Professor Xiao-Ping Dong, State Key Laboratory for Infectious Disease Prevention and Control, Collaborative Innovation Center for Diagnosis and Treatment of Infectious Diseases (Zhejiang University), National Institute for Viral Disease Control and Prevention, Chinese Center for Disease Control and Prevention, 155 Chang-Bai Road, Beijing 102206, P.R. China
E-mail: dongxp238@sina.com

*Contributed equally

Key words: scrapie, interspecies transmission, successive passage, glycosylation profile, neuropathology

Introduction

Prion diseases, also known as transmissible spongiform encephalopathies (TSEs), are a group of rapidly progressive neurodegenerative diseases that can affect different species, as well as humans, and include Creutzfeldt-Jakob disease (CJD) and Kuru in humans, bovine spongiform encephalopathy (BSE) in cattle, scrapie in sheep and chronic wasting disease (CWD) in cervids (1). It is widely accepted that prion diseases are caused by a type of unconventional infectious agents termed 'prions', which definitely differ from all known microorganisms as they lack any type of nucleic acid (2). The conformational conversion from a host-encoded glycoprotein termed 'PrP^{C}' into a misfolded conformer 'PrP^{Sc}', characterized by the change from high a α-helix to a high β-sheet content in the context of PrP secondary structure, is believed to be the critical event in prion propagation and the pathogenesis of prion disease. Prion infectivity largely lies on the prion protein itself, as only the procedures to modify or hydrolyze PrP^{Sc} are sufficient to 'clean up' its infectivity, while the methodologies to destroy nucleic acids do not affect prion infectivity (3). Another feature differing from other conventional infectious diseases is that no evidence exists for host specific immnuoresponse during prion pathogenesis, regardless of cellular or humoral immunity (4).

On the other hand, prion possesses two characteristics that are shared with other conventional infectious agents. One is the species barrier, which restricts or postpones the infection of a special prion across other species (5). The biological effect of the species barrier is reflected by complete resistance or low sensitivity with a longer incubation time in some animals when

inoculated with prion agents from other species. The species barriers of prion transmission can be overcome naturally or experimentally. A famous example is the outbreak of BSE that was believed to be caused by the contamination of scrapie agents in feed and subsequently induced the emergence of the human variant, CJD (vCJD) (6,7). The other is the existence of multiple prion strains, which renders a prion strain maintaining its specific and stable phenotypic traits following inoculation in the same host, such as incubation time, clinical manifestations, PrP^{Sc} patterns and neuropathological abnormalities. More than 20 strains of scrapie have been described to date (8).

In a previous study, we reported that 2 mouse-adapted scrapie strains, 139A and ME7, can overcome the species barrier to induce experimental scrapie in hamsters following long incubation times. Along with the establishment of interspecies transmissions, the major pathogenic characteristics of these 2 scrapie strains have changed (9). In the present study, in order to assess the possible changes of the infective and pathogenic characteristics of these 2 experimentally-formed scrapie strains during further passage, we re-inoculated them into hamsters. Following markedly short incubation periods, typical experimental TSE was induced in all the infected animals. The pathogenic and neuropathological characteristics of the 2nd passage infections were comparatively analyzed with their 1st passage strains and their original mouse-adapted strains.

Materials and methods

Scrapie strains. The hamster-adapted scrapie strain, 263K (263K-ha), and the mouse-adapted scrapie strains, 139A (139A-mo) and ME7 (ME7-mo), were intracerebrally passaged in respective rodents, whose clinical and neuropathological characteristics were described in our previous study (9). The experimental hamster-adapted scrapie strains, 139A (139A-ha) and ME7 (ME7-ha), were generated by interspecies nuclear transfer through the intracerebral infection of the agents, 139A-mo and ME7-mo, into hamsters, respectively, by prolonging the incubation periods (9).

Animal bioassay. Brain materials from the animals infected with the 1st passage of 139-ha and ME7-ha were homogenized (1:10) as inoculum prior to challenging. A total of 1 μl of individual brain homogenate was intracerebrally injected into 15-day-old Golden hamsters (obtained from Vital River Laboratories, Beijing, China) under halothane anaesthesia. For equilibrating the injected amounts of the different strains, we analyzed the absolute PrP^{Sc} gray values of different strains using western blots with the same loading volume following proteinase K (PK) digestion. Each group consisted of 8 female hamsters. The animals were monitored twice a week before the appearance of clinical signs determined by experienced staff, and once a day after the appearance of clinical symptoms until the animals died. The clinical symptoms and signs were scored as previously described (10). The incubation time was calculated from the inoculation to the onset of clinical manifestations and the clinical course was evaluated from the onset of the clinical manifestations to the time of death at the terminal stage of the disease. The main clinical manifestations at the final stages of the disease included progressive ataxia, sluggishness, loss of weight and extreme emaciation. At the end of the clinical phase, the animals were euthanized by ether and exsanguination and the brains were surgically removed from the hamsters for further testing.

Purification of PrP^{Sc} and PK digestion. The brain samples from the infected hamsters or mice were homogenized in 10% lysis buffer (100 mM NaCl, 10 mM EDTA, 0.5% Nonidet P-40, 0.5% sodium deoxycholate, 10 mM Tris, pH 7.5) according to a previously described protocol (11). Tissue debris was removed with low speed centrifugation at 2,000 g/min for 10 min and the supernatants were collected for further analysis. To detect the presence of PK-resistant PrP^{Sc} in the brain tissues, the brain homogenates were firstly digested with a final concentration of 50 μg/ml PK at 37˚C for 60 min prior to western blot analysis. To evaluate PK resistance to PrP^{Sc} from the various scrapie strains, the brain specimens were treated with various concentrations of PK at final concentrations of 100, 200, 500, 1,000 and 2,000 μg/ml at 37˚C for 60 min. PK digestion was terminated by heating the samples at 100˚C for 10 min.

Western blot analysis. Aliquots of the brain homogenates were separated on 12% SDS-PAGE and electroblotted onto nitrocellulose membranes using a semi-dry blotting system (Bio-Rad, Hercules, CA, USA). The membranes were blocked with 5% (w/v) non-fat milk powder (NFMP) in 1X Tris-buffered saline containing 0.1% Tween-20 (TBST) at room temperature for 1 h and then probed with individual primary antibodies at 4˚C overnight, including, anti-PrP monoclonal antibody (mAb) (6D11, sc-58581, Santa Cruz Biotechnology, Dallas, TX, USA) and anti-β-actin mAb (Sr-25113, Subrray Biotechnology). After washing with TBST, the blots were incubated with horseradish peroxidase (HRP)-conjugated goat anti-mouse or rabbit IgG (no. 31460 and no. 31430, Thermo Fisher Scientific, Waltham, MA, USA) at room temperature for 2 h. The blots were developed using an Enhanced ChemoLuminescence system (ECL, NEL103E001EA; PerkinElmer, Waltham, MA, USA) and visualized on autoradiography films. Images were captured using a ChemiDoc™ XRS+ Imager (Bio-Rad).

Deglycosylation assay. After mixing with equal volumes of glycoprotein denaturing buffer (New England Biolabs, Ipswich, MA, USA), the various brain homogenates were heated at 100˚C for 10 min. Subsequently, 50 mM sodium phosphate, pH 7.5, containing 1% NP-40 and 2 μl of N-glycosidase F (1,800,000 U/mg, New England Biolabs) were added to the samples and the mixtures were incubated at 37˚C for 2 h. PrP signals in each preparation were detected by western blot analysis as described above.

Pathological assays. The brain tissues from the hamsters infected with the different hamster-adapted strains were fixed in 10% buffered formalin solution. Prior to histological analysis, all the fixed tissues were immersed in 98% formic acid for at least 1 h for inactivation. Paraffin sections (5 μm) were subjected to conventional staining with hematoxylin and eosin (H&E). The spongiform degeneration in the brain regions infected with the various scrapie strains was monitored by light microscopy and the severity and distribution of vacuolation were measured according to a previously described protocol (12) as follows: 0, no lesions; 0.5, minimum vacuolation (2-3 vacuoles in half a x40 objective field); 1.0, little vacuolation (3-5 vacuoles in

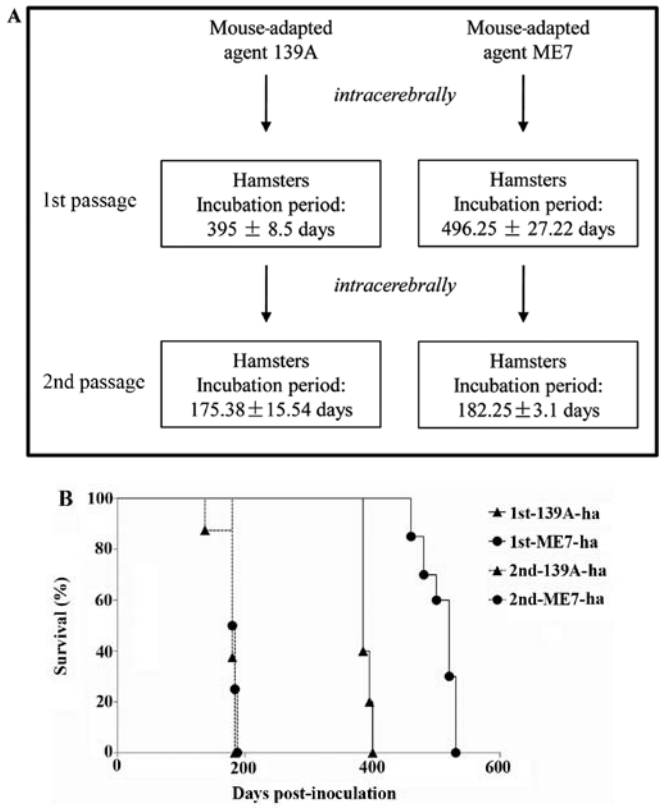

Figure 1. Intracerebral inoculation of the mouse-adapted scrapie strains, ME7-mo and 139A-mo, into hamsters. (A) Summarization of the interspecies transmissions of ME7-mo and 139A-mo into hamsters infected with the 1st and 2nd passage of the strains. (B) Comparative incubation times of the hamsters infected with the 1st and 2nd passage of the strains. The abscissa shows the survival days and the y-axis shows the percentages of survival.

half a field); 2.0, moderate vacuolation (several vacuoles evenly scattered); 3.0, extensive vacuolation (many vacuoles distributed in half a field); 4.0, severe vacuolation (numerous vacuoles often coalescing).

Immunohistochemistry (IHC). The brain tissues were fixed in 10% buffered formalin solution. Prior to histological analysis, all the fixed tissues were immersed in 98% formic acid for at least 1 h for inactivation of the infection. Paraffin sections (5 μm) of the brain tissues were prepared and IHC was performed according to a previously published protocol (10). Prior to the staining of PrP mAb, the brain sections were treated with 4 M guanidinium hydrochloride (GdnHCl) for 10 min. The sections were quenched for endogenous peroxidase in 3% H_2O_2 in methanol for 10 min and pre-treated with enzyme digestion antigen retrieval for 1 min. After blocking in 1% normal goat serum, the sections were incubated overnight at 4˚C with anti-PrP mAb (6D11) or anti-GFAP mAb, and rabbit anti-Iba1 polyclonal antibody (pAb). The sections were then incubated with HRP-conjugated goat anti-mouse or rabbit secondary antibody (no. 31460 and no. 31430, Thermo Fisher Scientific) for 60 min, and visualized by incubation with 3,3-diaminobenzidine tetrahydrochloride (DAB). The slices were counterstained with hematoxylin, dehydrated and mounted in permount.

Statistical analysis. Statistical analysis was performed using the SPSS 17.0 statistical package. Quantitative analysis of the western blots was carried out using ImageJ software The gray values of each target blot were evaluated. Statistical analyses were performed using the Student's t-test. A P-value <0.05 was considered to indicate a statistically significant difference.

Ethics statement. This study was approved by the Ethics Committee of the National Institute for Viral Disease Control and Prevention, China CDC under protocol 2009ZX10004-101.

Results

Subsequent passaging of the scrapie agents, 139A-ha and ME7-ha, in hamsters significantly shortens the incubation times. In our previous study, we demonstrated that the inoculation of 2 mouse-adapted scrapie strains, 139A-mo and ME7-mo, into hamsters successfully overcame the species barrier and induced experimental scrapie (9). In this study, in order to further stabilize these 2 newly-formed scrapie agents in hamsters, the pooled brain homogenates of the 1st passage 139A-ha (139A-ha.1st) and ME7-ha (ME7-ha.1st) were intracerebrally inoculated into 8 Golden hamsters (15 days old). One animal infected with agent 139A-ha.1st presented clinical symptoms at 137 days post-inoculation (dpi) and the remaining 7 animals presented with clinical manifestations at 180-184 dpi, with an average incubation of 176.1±15.9 days. The 8 animals infected with agent ME7-ha.1st became ill at 180-188 dpi, with an average incubation of 183.0±3.6 days. The incubation times of the 2nd passage of 139A-ha (139A-ha.2nd) and ME7-ha (ME7-ha.2nd) in the hamsters were quite comparable with those of their parent mouse strains in C57 mice (183.9±23.1 days for 139A-mo and 184.2±11.8 days for ME7-mo). Compared with the long incubation times of the 1st passage of the infection (395.0±8.5 days for 139A-ha and 496.3±27.2 days for ME7-ha), the incubation periods of the 2nd passage of 139A-ha and ME7-ha became much shorter (Fig. 1A). The survival times of the animals infected with the different scrapie agents, including 263K-ha, 139A-ha.1st, ME7-ha.1st, 139A-ha.2nd and ME7-ha.2nd are illustrated in Fig. 1B.

The most obvious clinical signs of those 2 experimental scrapie animals were quite similar, mainly consisting of progressive ataxia, sluggishness, loss of weight and extreme emaciation at the end stages of the disease. The clinical course of the 139A-ha.2nd-infected hamsters varied from 8-17 days, with an average of 14.9±3.0 days, while that of ME7-ha.2nd-infected hamsters was 15-17 days, with an average of 15.8±0.9 days (Table I). The clinical course of the 2nd passage-infected hamsters, regardless of infection with 139A-ha.2nd or ME7-ha.2nd, was similar (approximately 15 days), revealing different patterns compared with those of 1st passage infection (25-30 days for 139A-ha.1st and 30-40 days for ME7-ha.1st), as previously described (9).

PrP^{Sc} of the 2nd passage of 139A-ha and ME7-ha maintains the same biochemical characteristics as that of the 1st passage. We demonstrated that PrP^{Sc} of the mouse-adapted scrapie agents altered its glycosylation pattern from predominant monoglycosylated PrP^{Sc} to predominant diglycosylated PrP^{Sc} during cross-species infection in hamsters. In order to assess the glycosylation profiles of PrP^{Sc} in the brains of the hamsters infected with the 2nd passage strains, the brain homogenates

Table I. Incubation times and clinical courses of the hamsters infected with the scrapie strains, ME7 and 139A, at the 1st and 2nd passage.

Strain	Number (died from scrapie[a]/inoculated)	Incubation time (days) mean ± SD (range)	Clinical course (days) mean ± SD (range)
ME7-ha-1st[b]	6/6	496.3±27.2 (460-530)	33.8±3.9 (30-40)
139A-ha-1st[b]	5/5	395.0±8.5 (385-405)	26.8±1.9 (25-30)
ME7-ha-2nd	8/8	183.0±3.6 (180-188)	15.8±0.9 (15-17)
139A-ha-2nd	8/8	176.1±15.9 (137-184)	14.9±3.0 (8-17)

[a]Confirmed by brain PrP^{Sc} assays using western blot analysis and immunohistochemistry. [b]From our previous study by Shi *et al* (9).

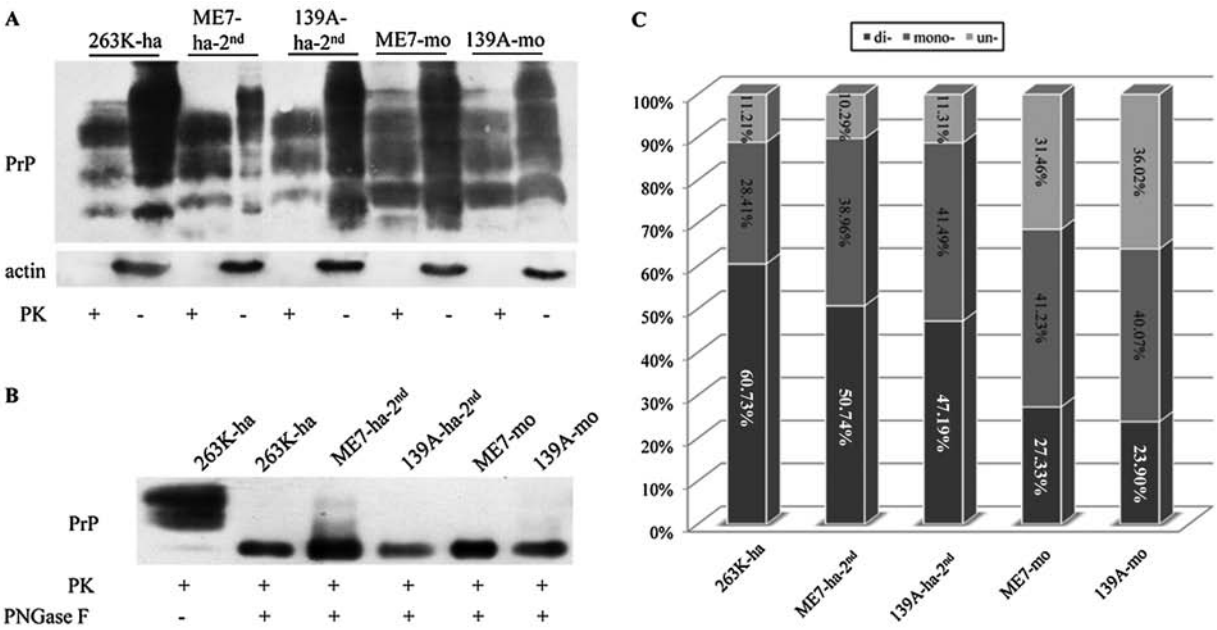

Figure 2. Western blot analysis for PrP^{Sc} in the brain homogenates of various scrapie-infected rodents. The PrP specific antibody used in western blot analysis was mAb 6D11. (A) Total PrP (PK-) and PrP^{Sc} (PK+) in the brains of hamsters infected with the strains, 263K-ha, ME7-ha-2nd and 139A-ha-2nd, and in the brains of mice infected with the strains, ME7-mo and 139A-mo (left panel), as well as in the brains of hamsters infected with the strains, ME7-ha-1st and 139A-ha-1st (right panel). (B) Deglycosylation PrP^{Sc} in the brains of animals infected with the strains, 236K, ME7-ha-2nd, 139A-ha-2nd, ME7-mo and 139A-mo; PrP^{Sc} not digested with PNGase F is shown on the left panel. (C) Quantitative analysis of the ratios of di-, mono- and unglycosylated PrP^{Sc} in the brains of animals infected with the various scrapie strains.

form the hamsters infected with ME7-ha.2nd and 139A-ha.2nd were subjected to PrP-specific western blot analysis, together with the hamster brains infected with a hamster-adapted agent [263K (263K-ha)] and the mouse brains infected with the mouse-adapted agents, ME7 (ME7-mo) and 139A (139A-mo). Following PK-digestion, 3 PK-resistant bands were observed in all preparations (Fig. 2A). The deglycosylation of the PrP^{Sc} molecules of ME7-ha.2nd and 139A-ha.2nd with PNGase F revealed a signal PrP-specific band at the same position, which also mobilized at the same position as the parent strains (ME7-mo and 139A-mo) and the strain of 263K-ha (Fig. 2B). Quantitative analysis of the 3 PK-resistant PrP bands in Fig. 2A revealed that similar to those of ME7-ha.1st and 139A-ha.1st, the PrP^{Sc} molecules of ME7-ha.2nd and 139A-ha.2nd were also predominantly diglycosylated, which were more similar to the hamster-adapted strain, 263K-ha, but obviously distinct from those of their original parent mouse-adapted strains, ME7-mo and 139A-mo (Fig. 2C).

Furthermore, PK resistance to various PrP^{Sc} molecules was evaluated by treatment with of various concentrations of PK (100-2,000 μg/ml). Under our experimental conditions, clear PK-resistant PrP bands were detectable in all preparations, even in the preparations of the highest dosage of PK (2,000 μg/ml) (Fig. 3A), indicating that the PrP^{Sc} molecules of ME7-ha.2nd and 139A-ha.2nd possessed strong PK resistance to PrP^{Sc}. Analyses of the intensities of PK-resistant PrP signals revealed a comparable level of the PrP^{Sc} molecules of ME7-ha.2nd and 139A-ha.2nd in all preparations, which were also comparable with the PrP^{Sc} molecules in the brains of 263K-infected hamsters, but clearly stronger than those in the brains of ME7-mo- and 139A-mo-infected mice (Fig. 3B).

Large quantities of PrP^{Sc} deposited in the brains of animals infected with ME7-ha.2nd and 139A-ha.2nd. To determine the characteristics of PrP^{Sc} deposits in the brains of the hamsters infected withthe 2nd passage strains, brain slices of the cortex

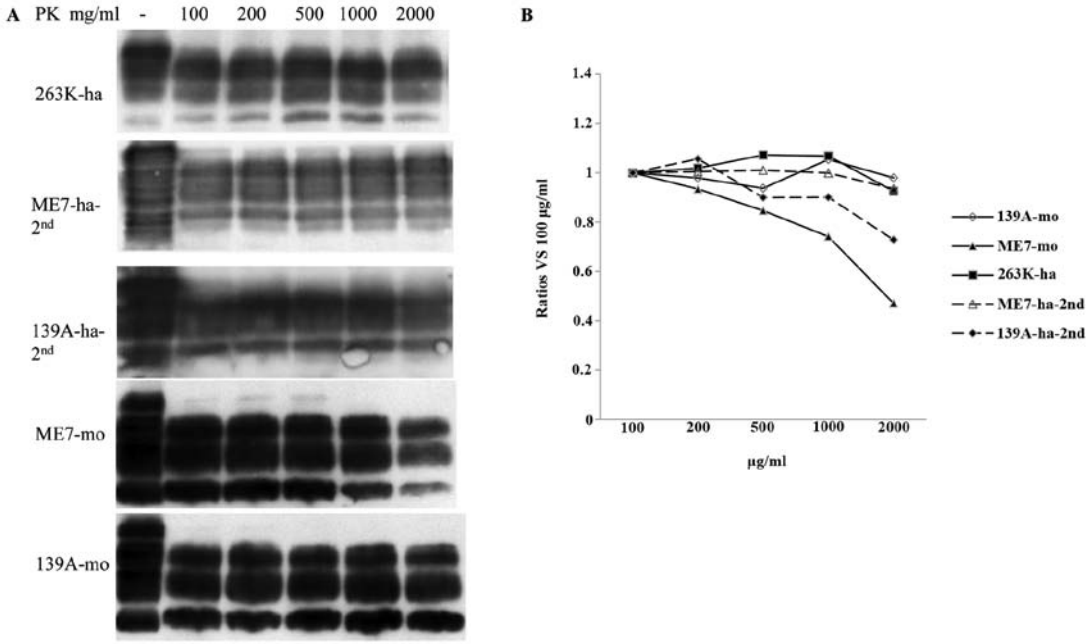

Figure 3. PK resistance to PrP^{Sc} in the brains of rodents infected with the various agents. (A) Western blot analysis with mAb 6D11. The concentrations of PK in individual preparations are indicated on the top. (B) Quantitative analyses of each gray numerical value of the PrP blots. Relative gray values of the PrP signals in each experiment were normalized by division with those of the respective reaction without PK.

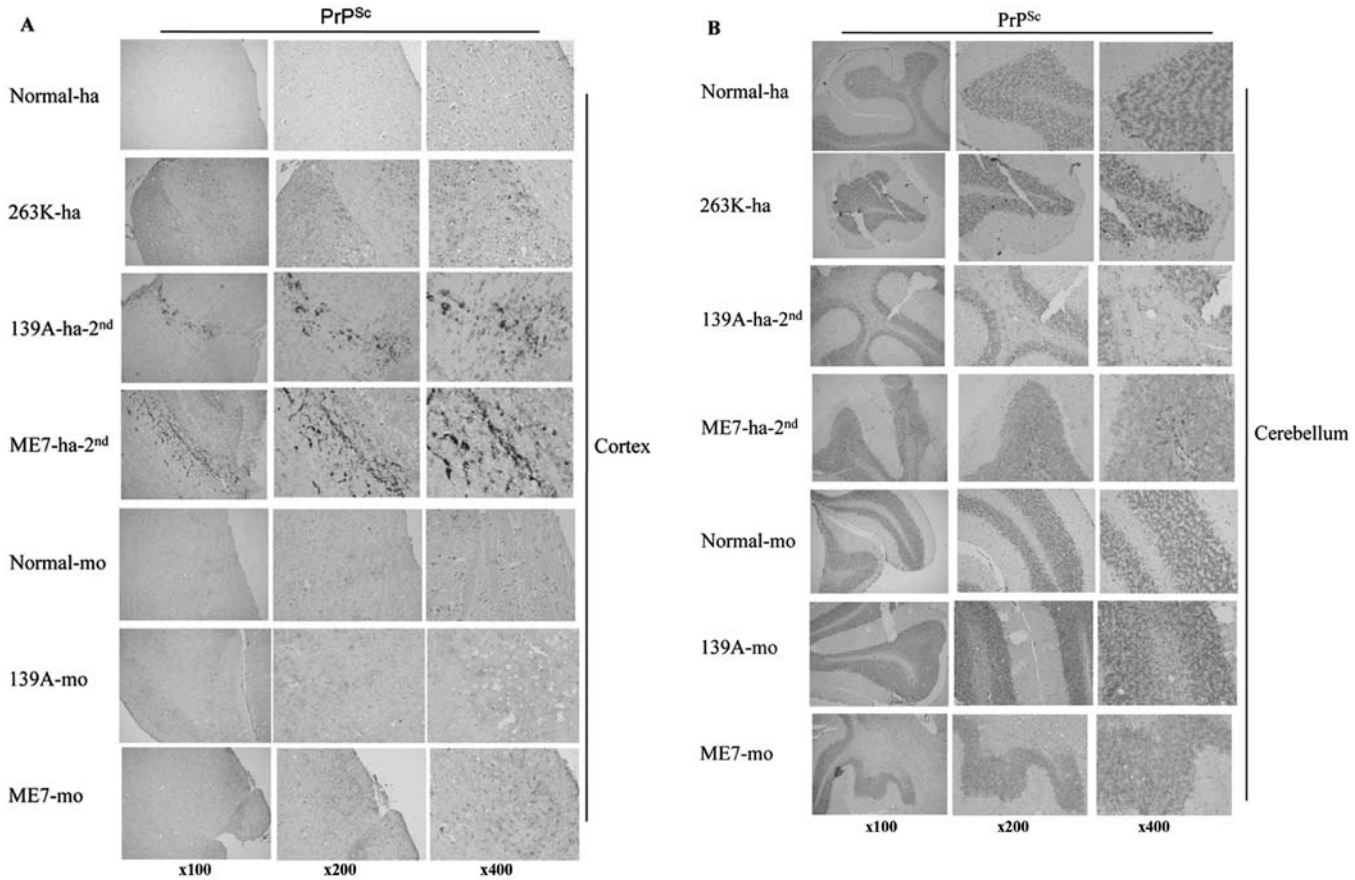

Figure 4. Immunohistochemistry for PrP^{Sc} deposits in the brains of animals infected with the various strains using mAb 6D11. Age-matched normal hamsters and mice were used as normal controls. Brain sections were treated with GdnHCl prior to reaction with mAb 6D11. (A) Cortex. (B) Cerebellum. The magnifications are shown on the bottom.

and cerebellum from the ME7-ha.2nd- and 139A-ha.2nd-infected hamsters were comparatively analyzed with those from the 263K-infected hamsters, as well as those from the ME7-mo- and 139A-mo-infected mice by PrP^{Sc}-specific IHC.

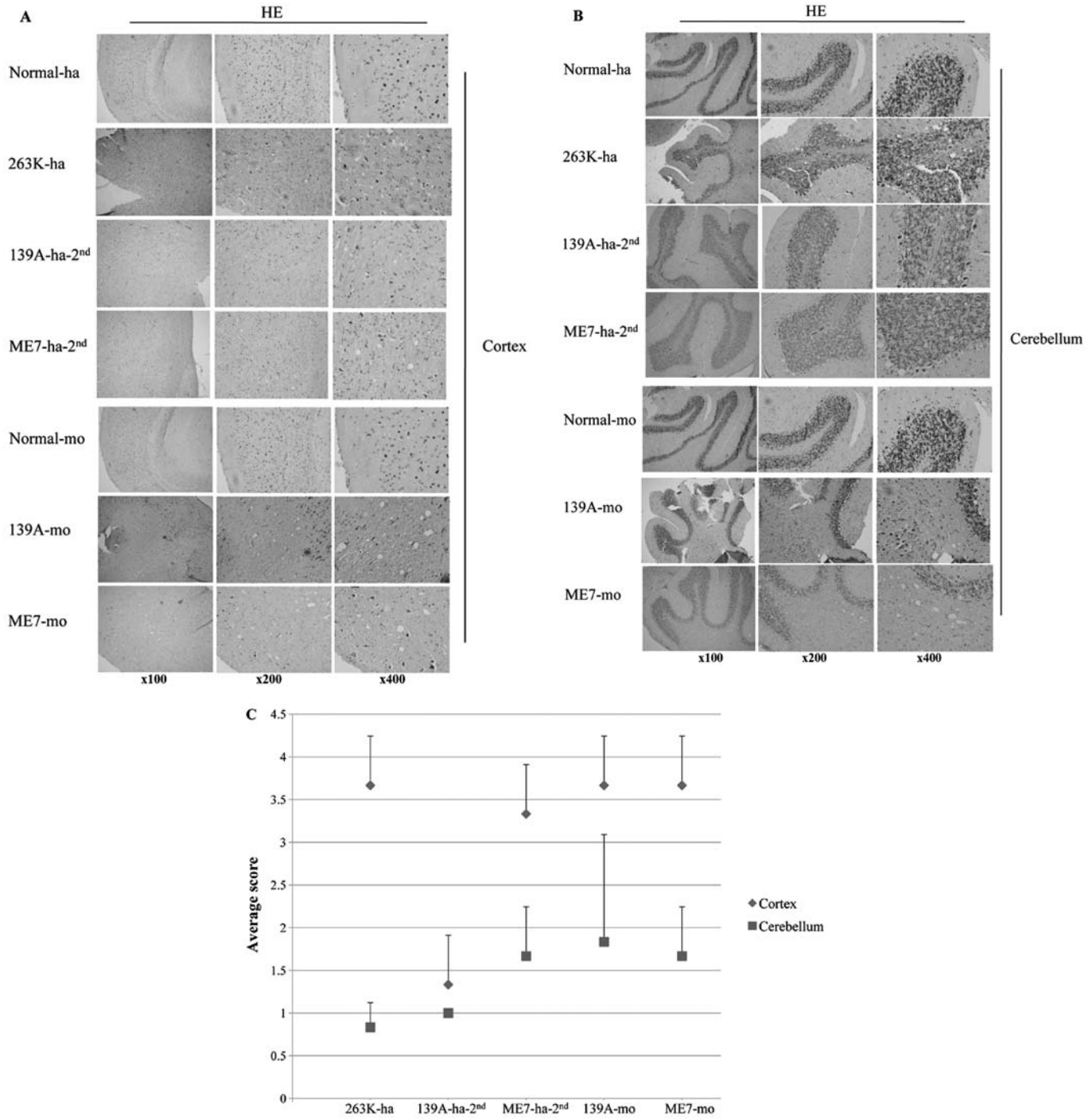

Figure 5. H&E staining of the brain tissue of animals infected with the strains, 263K-ha, ME7-ha-2nd, 139A-ha-2nd, ME7-mo and 139A-mo. (A) Cortex. (B) Cerebellum. The magnifications are shown on the bottom. (C) Scores of the severity and distribution of vacuolation. The average value for each brain region was calculated from 3 independent counts and is indicated as the mean ± SD.

Following treatment with 4 M GdnHCl at 4˚C for 2h and staining with PrP mAb (6D11), large amounts of plaque PrP^{Sc} deposits were detected in the cortex regions of the ME7-ha- and 139A-ha-infected animals, revealing a greater number of and larger plaque-like deposits compared with the of 263K-infected hamsters (Fig. 4A). By contrast, the PrP^{Sc} deposits in the cortex regions from the ME7-mo- and 139A-mo-infected mice revealed typical synaptic patterns, lacking the accumulation of large plaques (Fig. 4A). Compared with the observations in the cortex, the number of deposits of PrP^{Sc} in the cerebellum regions of all the tested animals were markedly less, presenting in a punctate and/or dispersive manner (Fig. 4B). Compared with the other strains, a greater number of PrP deposits were observed in the cerebellum of the ME7-ha-infected animals, particularly in the region of the cerebellar medulla.

Spongiform changes in the brain tissues of ME7- and 139A-infected hamsters and mice. Neuropathological assays of the cortex (Fig. 5A) and cerebellum (Fig. 5B) regions of ME7-ha.2nd- and 139A-ha.2nd-infected hamsters revealed

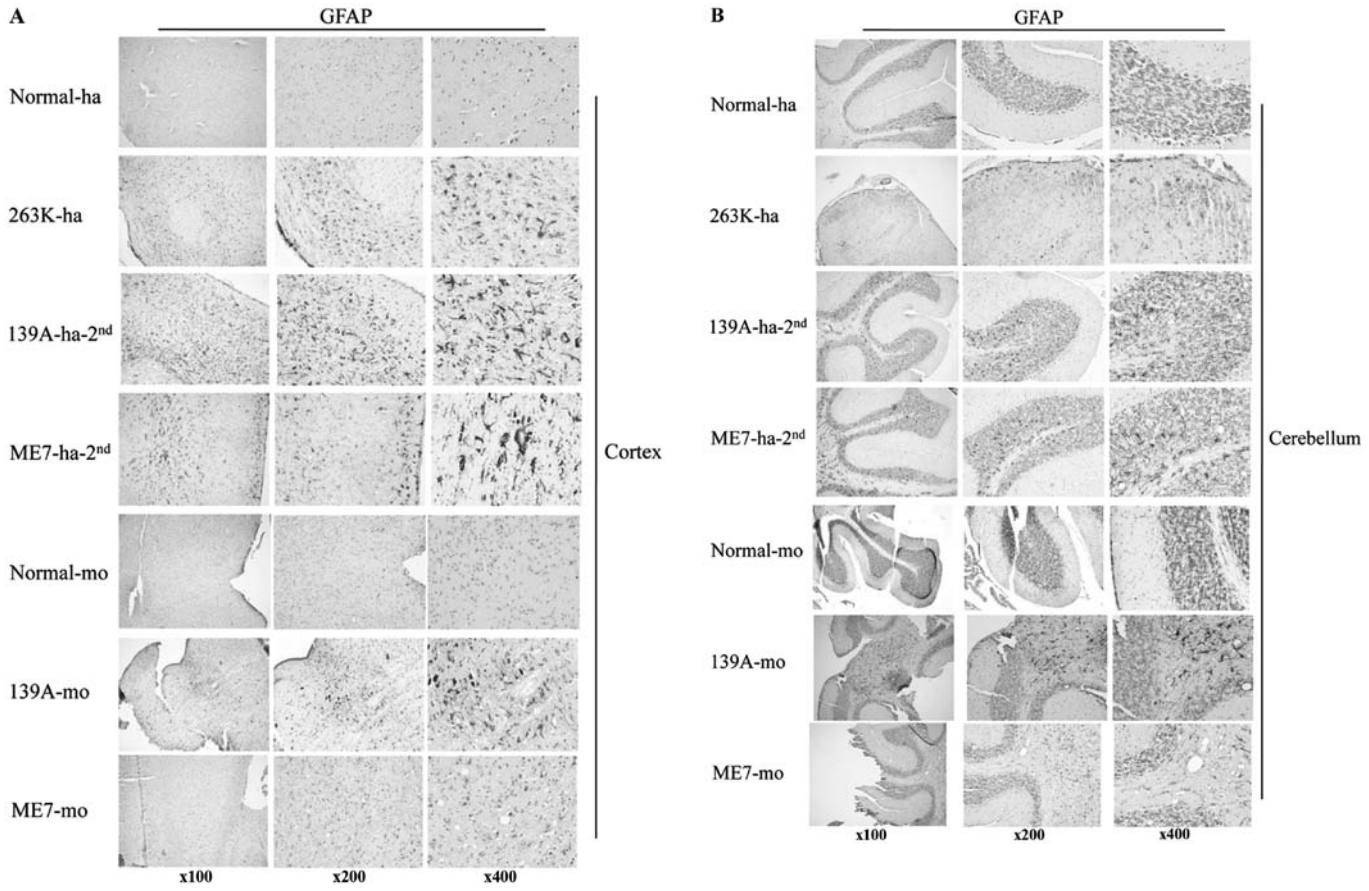

Figure 6. GFAP-specific immunohistochemistry of the brain tissues of animals infected with the various strains. (A) Cortex. (B) Cerebellum. The magnifications are shown on the bottom.

numerous vacuoles in the fields of vision. Most of the vacuoles were round or oval with different sizes. Obvious spongiform degenerations were also observed in the brain sections of the mice infected with the parent mouse strains, ME7 and 139A (Fig. 5A and B). The severity and distribution of vacuolation in the cortex and cerebellum of the animals infected with the various strains were calculated by semiquantitative analysis. In the cortex regions, the average lesion scores of the 263K-ha-, 139A-ha.2nd-, ME7-ha.2nd-, 139A-mo- and ME7-mo- animals were 3.7, 1.3, 3.3, 3.7 and 3.7, respectively, while in the cerebellum regions, the average lesion scores were 0.8, 1.0, 1.7, 1.8 and 1.7, respectively (Fig. 5C). It seems that the vacuolation of the ME7-infected rodents, either hamsters or mice, is more frequently viewed than that of 139A-infected ones.

Marked astrogliosis and microglia proliferation in the brain tissues of ME7- and 139A-infected rodents. To further analyze gliocyte proliferation, the brain sections were used for GFAP- and Iba1-specific IHC tests. Abundant large GFAP positive-stained astrocytes were observed in the regions of the cortex (Fig. 6A) and cerebellum (Fig. 6B) of the ME7-ha.2nd- and 139A-ha.2nd-infected hamsters, which were more obvious than those in the brains of mice infected with the parent strains, ME7-mo and 139A-mo. Astrogliosis in the cortex regions was more notable than in the cerebellum regions of all the infected animals tested. Iba1-specific IHC assays identified an abundance of microglia with a greater number of larger round- or amoeboid-shaped cell bodies in the brain sections of the ME7-ha.2nd- and 139A-ha.2nd-infected animals, without significant differences observed between the regions of the cortex and cerebellum, or between the hamster-adapted strains and the mouse-adapted strains (Fig. 7A and B).

Discussion

In this study, we successively passaged our previously generated cross-species hamster-adapted strains [ME7-ha and 139A-ha (9)] using the same experimental host hamsters. Compared with the extremely long incubation times of the 1st passage of the strains ME7-ha (496.3±27.2 days) and 139A-ha (395.0±8.5 days), the incubation periods of the 2nd passage of those 2 strains were markedly shorter. Such a phenomenon is a common occurence in experimental prion infection when passaging a prion strain into a new host; the incubation time shortens during successive passaging (13,14). Of note, the incubation times of the 2nd passage of the 2 strains in hamsters were quite comparable with those of their parent strains in mice, but much longer than those of another hamster-adapted strain, 263K-ha (66.7±11.0 days) (15). Although the exact element that determines the incubation time remains unknown, it seems that besides the original prion strain, the new host environment may also largely influence the incubation time (16). In addition, the clinical courses of the ME7-ha.2nd- and 139A-ha.2nd-infected hamsters were also shorter than those of the hamsters infected

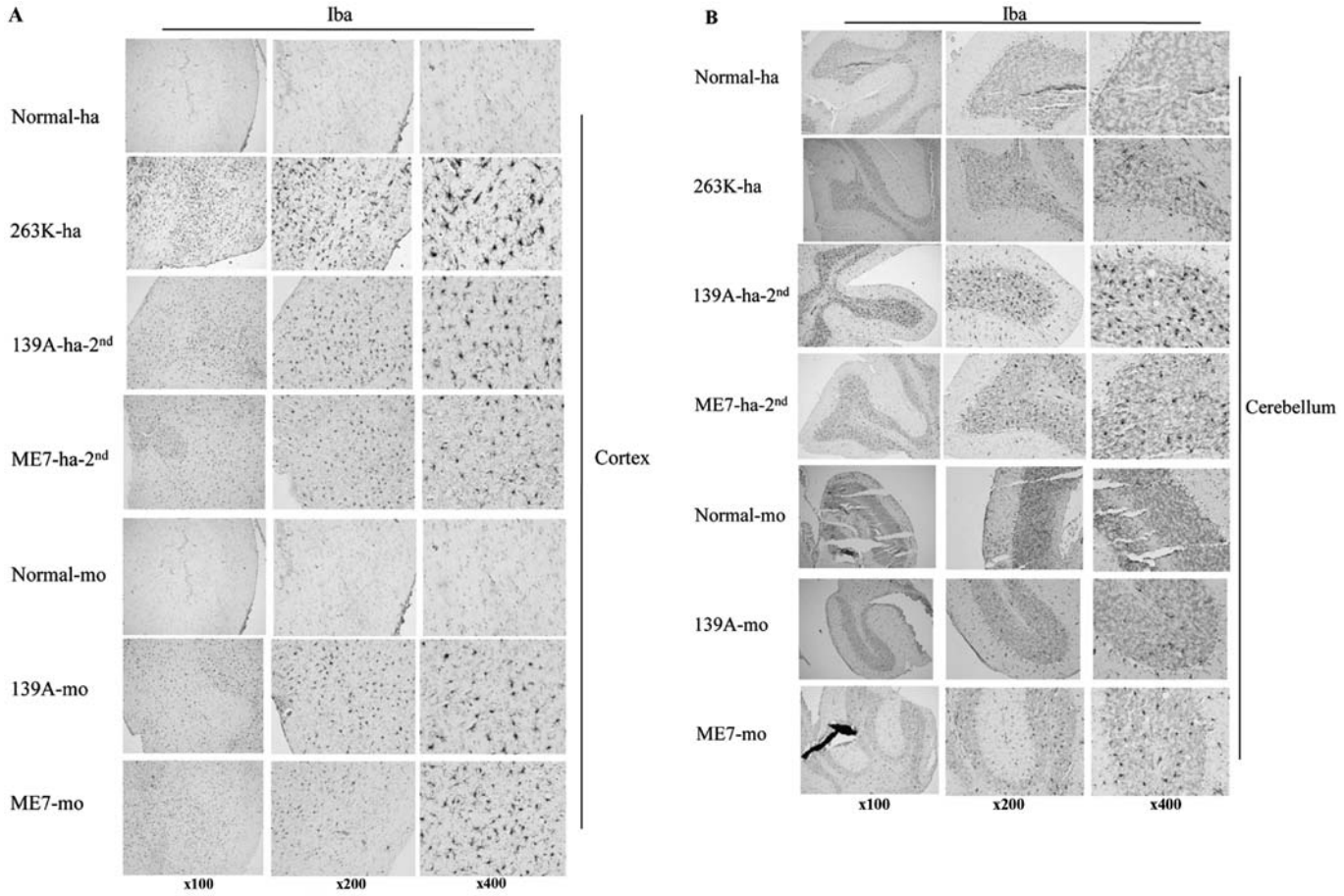

Figure 7. Iba-specific immunohistochemistry of the brain tissue of animals infected with the various strains. (A) Cortex. (B) Cerebellum. The magnifications are shown on the bottom.

with the 1st passage of the strains. This indicated that the 2nd passage of the experimentally-generated scrapie strains became more adaptable to the environment of the new host. Further continuous passaging of the ME7-ha and 139A-ha strains into hamsters may help these 2 new scrapie strains to become more stable and mature in the new host.

The electrophoresis and glycosylation pattern of PrP^{Sc} are another index for distinguishing prion strains (17). Similar to the PrP^{Sc} molecules in the brain tissues of the hamsters infected with the 1st passage of the strains, the glycosylation patterns of the PrP^{Sc} molecules in the brains of the hamsters infected with the 2nd passage of the strains, ME7-ha and 139A-ha, were also predominantly diglycosylated, and were are totally distinct from those of their mouse-adapted parent strains (ME7-mo and 139A-mo) with predominantly monoglycosylated PrP^{Sc} in the infected mouse brains. This suggests that the PrP^{Sc} molecular characteristics, at least the glycosylation profile, of the newly-formed prion strains by interspecies infection is maintained during successive or serial passaging in the same host (18). Obviously, the molecular characteristics of PrP^{Sc} generated by interspecies infection are marked with the properties of the new host. The 1st or the 2nd passage of the strains, ME7-ha and 139A-ha, showed similar glycosylation profiles as those of hamster-adapted 263K, although the incubation time of the latter was much shorter. These data strongly suggest that the brain microenvironment of a new host, at least hamsters, obviously affects the PrP^{Sc} properties during cross-species transmission. In addition, the formation of PrP^{Sc} molecular characteristics occurs at the very early stage, as the glycosylation patterns of PrP^{Sc} are the same among the brain samples collected at the early, mid and terminal terms during infection with the 1st passage of ME7-ha and 139A-ha (9). In another study of ours on protein misfolding cyclic amplification (PMCA) (Gao *et al*, unpublished data), we illustrate that mouse-adapted agent 139A can efficiently induce the formation of PK-resistant PrP (PrP^{res}) when using hamster brain and muscle homogenates as the substrates, accompanied by the same shift in PrP^{res} glycosylation patterns as in the interspecies infection *in vivo* (19). Of note, such a shift in PrP^{res} glycosylation patterns is observed in the 1st round of PMCA and stably maintained in the subsequent rounds. One may speculate that the formation of the new molecular characteristics of PrP^{Sc} occur at the early stage of the interaction between mouse PrP^{Sc} and hamster PrP^{C}.

Typical neuropathological changes of experimental TSE were identified in the infection of the 2nd passage of stains ME7-ha and 139A-ha in hamsters, including spongiform degeneration, PrP^{Sc} deposits, astrogliosis and microglia proliferation. Quite comparable spongiform degeneration between the mouse and hamster strains highlights a similar brain damage in the central nerve system. Similar microglia proliferations that are commonly observed in the brains of the naturally occurring sporadic CJD (20) and experimentally

scrapie-infected rodents (21) reflect an activation of the innate immune system during prion infection. Similar to the existence of the differences in clinical and PrP^{Sc} molecular aspects, our neuropathological assays also revealed some strain-associated characteristics. PrP^{Sc} deposits in the brain, particularly in the cortex regions, presented distinct profiles between the hamster and mouse strains, with large amounts of plaque-like deposits in the hamster strains, while dispersive synapse-like accumulations were observed with the mouse strains. More severe astrogliosis was also observed in the cortex and cerebellum of the hamsters infected with the hamster strains. Certainly, we cannot simply exclude the possibility of the differences in the immunoreactivity to the antibodies used in our experiments between these 2 rodents, which may contribute to the diversity in IHC assays. Nevertheless, the different neuropathological profiles may also become one of the special characteristics of the hamster strains generated by cross-species infection.

The susceptibility of prion transmission is believed to be dependent largely on the homology of PrP^{C} proteins (22). The polymorphism of codon 129 of host PrP protein influences the susceptibility of prion infection, either in the interspecies transmission, such as from BSE to the human variant CJD (23), or in the intraspecies transmission, such as scrapie in sheep (24). However, transgenic mice assays have illustrated some exceptions for the determination of the PrP homology between the exotic prion (PrP^{Sc}) and host PrP^{C} in disease susceptibility, e.g., infection with the BSE agent in transgenic mice with bovine PrP gene surprisingly led to a longer incubation period than in wild-type mice (25), and heterozygote transgenic mice expressing human and murine PrP genes are more susceptible to a number of sCJD agents than homozygote transgenic mice expressing human PrP gene (26). Only 7 amino acids differences between hamster and mouse PrP proteins enable the efficient transmission of experimental scrapie from mice to hamsters, but this is extremely difficult from hamsters to mice (27). Obviously, apart from the PrP gene, there are some unknown factors, either in the host microenvironment or in the PrP protein itself, participating in the control of the susceptibility to prion infection. Additionally, host PrP^{C} and the microenvironment may also determine the molecular and pathological properties of new strains generated by interspecies prion transmission.

Acknowledgements

This study was supported by the China Mega-Project for Infectious Disease (2011ZX10004-101, 2012ZX10004215), Chinese National Natural Science Foundation Grants (81100980, 81301429), the Young Scholar Scientific Research Foundation of China CDC (2012A102) and the SKLID Development Grant (2012SKLID102, 2011SKLID104 and 2011SKLID211).

References

1. Liberski PP: Historical overview of prion diseases: a view from afar. Folia Neuropathol 50: 1-12, 2012.
2. Prusiner SB: The prion diseases. Brain Pathol 8: 499-513, 1998.
3. Colby DW and Prusiner SB: Prions. Cold Spring Harb Perspect Biol 3: a006833, 2011.
4. Wisniewski T and Goni F: Immunomodulation for prion and prion-related diseases. Expert Rev Vaccines 9: 1441-1452, 2010.
5. Hagiwara K, Hara H and Hanada K: Species-barrier phenomenon in prion transmissibility from a viewpoint of protein science. J Biochem 153: 139-145, 2013.
6. Ducrot C, Arnold M, de Koeijer A, Heim D and Calavas D: Review on the epidemiology and dynamics of BSE epidemics. Vet Res 39: 15, 2008.
7. Hagiwara K, Yamakawa Y and Hanada K: Acquired human prion diseases - past and present issues. Uirusu 59: 155-165, 2009 (In Japanese).
8. Solforosi L, Milani M, Mancini N, Clementi M and Burioni R: A closer look at prion strains: characterization and important implications. Prion 7: 99-108, 2013.
9. Shi Q, Zhang BY, Gao C, *et al*: Mouse-adapted scrapie strains 139A and ME7 overcome species barrier to induce experimental scrapie in hamsters and changed their pathogenic features. Virol J 9: 63, 2012.
10. Zhang J, Chen L, Zhang BY, *et al*: Comparison study on clinical and neuropathological characteristics of hamsters inoculated with scrapie strain 263K in different challenging pathways. Biomed Environ Sci 17: 65-78, 2004.
11. Gao JM, Gao C, Han J, *et al*: Dynamic analyses of PrP and PrP(Sc) in brain tissues of golden hamsters infected with scrapie strain 263K revealed various PrP forms. Biomed Environ Sci 17: 8-20, 2004.
12. Deleault NR, Harris BT, Rees JR and Supattapone S: Formation of native prions from minimal components in vitro. Proc Natl Acad Sci USA 104: 9741-9746, 2007.
13. Sweeting B, Khan MQ, Chakrabartty A and Pai EF: Structural factors underlying the species barrier and susceptibility to infection in prion disease. Biochem Cell Biol 88: 195-202, 2010.
14. Kimberlin RH and Walker CA: Evidence that the transmission of one source of scrapie agent to hamsters involves separation of agent strains from a mixture. J Gen Virol 39: 487-496, 1978.
15. Meade-White KD, Barbian KD, Race B, *et al*: Characteristics of 263K scrapie agent in multiple hamster species. Emerg Infect Dis 15: 207-215, 2009.
16. Luers L, Bannach O, Stohr J, *et al*: Seeded fibrillation as molecular basis of the species barrier in human prion diseases. PLoS One 8: e72623, 2013.
17. Aguzzi A, Heikenwalder M and Polymenidou M: Insights into prion strains and neurotoxicity. Nat Rev Mol Cell Biol 8: 552-561, 2007.
18. Beck KE, Thorne L, Lockey R, *et al*: Strain typing of classical scrapie by transgenic mouse bioassay using protein misfolding cyclic amplification to replace primary passage. PLoS One 8: e57851, 2013.
19. Siso S, Chianini F, Eaton SL, *et al*: Disease phenotype in sheep after infection with cloned murine scrapie strains. Prion 6: 174-183, 2012.
20. Shi Q, Xie WL, Zhang B, *et al*: Brain microglia were activated in sporadic CJD but almost unchanged in fatal familial insomnia and G114V genetic CJD. Virol J 10: 216, 2013.
21. Xie WL, Shi Q, Zhang J, *et al*: Abnormal activation of microglia accompanied with disrupted CX3CR1/CX3CL1 pathway in the brains of the hamsters infected with scrapie agent 263K. J Mol Neurosci 51: 919-932, 2013.
22. Greenlee JJ, Nicholson EM, Smith JD, Kunkle RA and Hamir AN: Susceptibility of cattle to the agent of chronic wasting disease from elk after intracranial inoculation. J Vet Diagn Invest 24: 1087-1093, 2012.
23. Saba R and Booth SA: The genetics of susceptibility to variant Creutzfeldt-Jakob disease. Public Health Genomics 16: 17-24, 2013.
24. Padilla D, Beringue V, Espinosa JC, *et al*: Sheep and goat BSE propagate more efficiently than cattle BSE in human PrP transgenic mice. PLoS Pathog 7: e1001319, 2011.
25. Wilson R, Hart P, Piccardo P, *et al*: Bovine PrP expression levels in transgenic mice influence transmission characteristics of atypical bovine spongiform encephalopathy. J Gen Virol 93: 1132-1140, 2012.
26. Asante EA, Gowland I, Grimshaw A, *et al*: Absence of spontaneous disease and comparative prion susceptibility of transgenic mice expressing mutant human prion proteins. J Gen Virol 90: 546-558, 2009.
27. Campbell S, Dennehy U and Telling G: Analyzing the influence of PrP primary structure on prion pathogenesis in transgenic mice. Arch Virol Suppl: 16: 87-94, 2000.